ACS Sustainable Chemistry & Engineering

pubs.acs.org/journal/ascecg

Research Article

Development and Production of Moderate-Thermophilic PET Hydrolase for PET Bottle and Fiber Recycling

Takashi Matsuzaki,♦ Toshiyuki Saeki,♦ Fuhito Yamazaki, Natsuka Koyama, Tatsunori Okubo, Daiki Hombe, Yui Ogura, Yoshihito Hashino, Rie Tatsumi-Koga, Nobuyasu Koga, Ryota Iino, and Akihiko Nakamura*

Cite This: *ACS Sustainable Chem. Eng.* 2025, 13, 10404−10417

Read Online

ACCESS | Metrics & More | Article Recommendations | Supporting Information

ABSTRACT: Polyethylene terephthalate (PET) is a widely utilized synthetic polymer found in bottles, textiles, and packaging materials. To enhance the activity of PET hydrolase PET2, seven new mutations were identified through random screening and combined with a previously reported variant, PET2-7M, to generate PET2-14M. In addition, two mutations that enhanced the positive charge on the binding surface of PET were identified. Concurrently, the substrate binding site of PET2-14M was modified using HotPETase as a structural reference, yielding PET2-14M-6Hot. Subsequently, the two mutations were introduced into PET2-14M-6Hot, considering the optimization screening results, and positively charged mutations were also combined. The final variant, PET2-21M, demonstrated a 28.6-fold increase in the concentration of total product compared with the PET2 wild-type. Expression systems for PET2-14M-6Hot and PET2-21M were established in*Komagataella phaffii*, producing up to 691 mg L^{-1} of PET2-14M-6Hot after 137 h of cultivation. PET2-21M (5 mg L^{-1}) completely degraded 20 g L^{-1} powder of commercial PET bottles within 24 h at 60 °C. Furthermore, PET2-14M-6Hot showed twice the degradation rate of LCC-ICCG on PET fiber and PET/cotton-blended fiber and achieved 2.2 times higher product yield than LCC-ICCG on PET/PU-blended fiber at 50 °C. These engineered PET2 variants could be candidates for recycling both pure and blended PET fibers under moderate-temperature conditions.

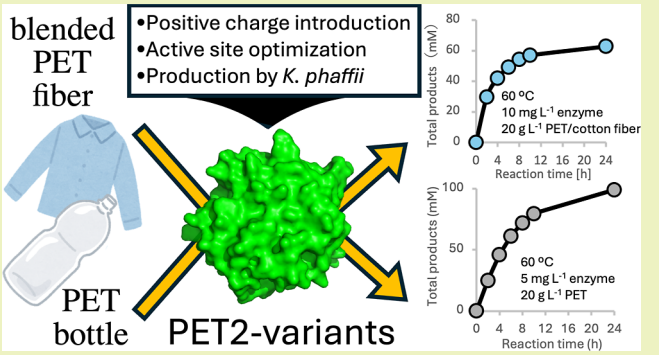

KEYWORDS: *PET hydrolase, polyethylene terephthalate, protein engineering, PET recycling, blended fiber degradation, polyurethane, Komagataella phaffii*

1. INTRODUCTION

Polyethylene terephthalate (PET) is a synthetic polymer consisting of terephthalic acid (TPA) and ethylene glycol (EG), alternately connected by ester bonds. PET demonstrates notable heat and abrasion resistance, as well as gas barrier properties, and is the sixth most widely produced plastic, surpassed by commodity plastics such as polyethylene (PE) and polypropylene (PP).[1] PET is employed in various forms, including films and fibers.

As a synthetic fiber, polyester accounts for 83% of the fiber market,[2] with more than 50 million tons of PET fibers produced in 2016.[3] Textile consumption is increasing, as exemplified by the fast fashion trend and textile waste,[4] and the associated resource consumption and emissions are expected to increase by 50% by 2030.[5] Therefore, methods to recycle low-quality waste fibers back into fibers are highly desirable from both the environmental and economic perspectives.[6] PET fibers are often blended with other polymers, such as cotton and polyurethane (PU), which complicates recycling. While mechanical separation is one approach, selective chemical degradation of PET offers greater material purity and recycling potential.[7] Nevertheless, recycling blended fibers remains one of the most challenging tasks due to the difficulty of isolating PET from composite materials.[8] Although mechanical deconstruction is possible, it typically results in quality loss (downcycling).[9] If each fiber component in a blend could be degraded selectively and independently, cross-contamination of degradation products could be avoided, thus improving the recyclability.

PET presents notable advantages in terms of recyclability, aligning with increasing environmental consciousness and the demand for sustainable plastics. PET recycling can be

Received: February 20, 2025
Revised: June 18, 2025
Accepted: June 18, 2025
Published: June 27, 2025

categorized into two methods: mechanical and chemical recycling.[10] Mechanical recycling is a cost-effective method that has been applied for practical use in beverage-bottle recycling systems. The inherent limitations of mechanical recycling are a decrease of the degree of polymerization and its inability to completely remove impurities, which results in a decrease in strength and discoloration.[11] Moreover, mechanical recycling is typically unsuitable for blended materials. In contrast, chemical recycling involves depolymerizing PET into its monomeric components, enabling the production of materials nearly equivalent to virgin PET.[12] While some solid catalysts can rapidly depolymerize PET at high temperatures (>180 °C), such processes often require harsh conditions and pose environmental risks.[13] Soluble catalysts such as potassium carbonate, using dichloromethane and methanol as solvents, were used to catalyze the methanolysis of PET at 25 °C.[14] But Tollini et al. reported that conversion of PET/cotton blended fiber was inhibited by the hydroxyl group of cellulose and moisture on the fiber.[15] Almost 100% TPA was recovered from polycotton (PET and cotton fiber) after 40 min of incubation, but the reaction temperature was 90 °C and 52 mmol kg^{-1} benzyl tributyl ammonium chloride and 10% (w/v) sodium hydroxide were used.[7] Tanaka et al. used dimethyl carbonate as the acceptor of EG, and lithium methoxide was used to catalyze the methanolysis of PET at 25−50 °C.[16] Using EG and tetrahydrofuran as solvents, PET was hydrolyzed by KOH at 60 °C for 1 h.[17] These methods are superior to mechanical recycling in terms of material quality, but they require large quantities of toxic and flammable reagents, so they are inferior in terms of environmental considerations.[18]

In this context, enzymatic depolymerization of PET provides a milder and more environmentally friendly alternative operating at temperatures below 80 °C and neutral pH in aqueous conditions. PET hydrolases are classified into two types: type I, derived from fungi, and type II, derived from bacteria.[19] The PET hydrolases have an α/β hydrolase fold and catalytic triad (Ser-His-Asp) at the catalytic center, like that of serine protease. Cutinases, which are the hydrolases of the wax layer of plants, are applied in the textile and detergent industries for fiber modification and removal of hydrophobic stains, contributing to more eco-friendly processing methods.[20] The first enzyme reported to degrade PET fibers was a cutinase from *Thermobifida fusca*,[21] and cutinase is also an enzyme with high potential industrial applications in PET enzymatic degradation.[19] Problems with enzyme catalysis include the low rate of reaction and limited accessibility to the crystal region of PET.[18] To solve this problem, high-activity variants of PET-hydrolyzing enzymes have been developed.[19] The most well-known variant is LCC-ICCG, a variant derived from leaf and branch compost cutinase (LCC), which was reported in 2020.[22] 90% depolymerization of 200 g of PET per kilogram of reaction mixture was achieved by LCC-ICCG in 9.3 h at pH 8 and 72 °C, and the maximum specific space-time yield was 70.1 g-TPA L^{-1} h^{-1} g-enzyme^{-1}. LCC-A2, which was a variant of LCC-ICCG developed with affinity analysis based on dynamic docking, showed the maximum specific space-timeyield was 110.75 g-TPA L^{-1} h^{-1} g-enzyme^{-1} against cryo-milled postconsumer PET.[23]

PETase from *Ideonella sakaiensis* (IsPETase) is one of the major origins of variants such as ThermoPETase,[24] DuraPETase,[25] FastPETase,[26] HotPETase,[27] and TurboPETase.[28] ThermoPETase (500 nM) produced 100 μM products from a PET film at pH 9.0 and 40 °C after incubation for 3 days. DuraPETase (0.05 mg mL^{-1}) produced 3.1 mM products from a PET film at pH 9.0 and 40 °C after 3 days. FastPETase (200 nM) was mixed with 25 mg of a PET film in 600 μL of potassium phosphate buffer (pH 8.0), producing 32.8 mM products at 50 °C for 24 h. HotPETase (40 nM) degraded 4 mg mL^{-1} crystalline-PET powder and released about 3 mM products after 48 h of incubation at pH 9.2 and 40 °C. The activities of four enzymes (FastPETase, HotPETase, PES-H1L92F/Q94Y, and LCC-ICCG) were compared against 165 g per kg of postconsumer waste PET at their optimized reaction conditions, and LCC-ICCG still showed the best performance.[29] TurboPETase completely hydrolyzed 200 g of a pretreated PET bottle with 400 mg of enzyme per kg reaction mixture at pH 8.0 and 65 °C for 8 h, exhibiting higher depolymerization activity than LCC-ICCG, which was tested at both 65 and 72 °C.

High reaction specificity is a characteristic of enzymes, but there are still few papers that investigate the degradation of blended fibers. Mixed fibers of PET and cotton were ball-milled with commercially available cutinase from *Humicola insolens* (HiC) and a cellulase mixture (CTec2), and 14 ± 1% of PET was degraded after 7 days at 55 °C[8]. The performances of the enzymes are summarized in Table S1.

PET2, a lipase found in the metagenome library of a gelatin-enriched fed-batch reactor,[30] lacks the lid structure, which is an important feature for lipase activity and substrate selectivity.[31] Recently, PET2 has been reported to be a PET hydrolase.[32] We previously reported the development of PET2-7M (PET2-R47C-G89C-F105R-E110K-S156P-G180A-T297P), a thermostable and active variant of PET2.[33] The structure of PET2 was stabilized by computationally estimated mutations and an additional disulfide bond, and the effects were evaluated by determining its X-ray crystal structure (PDB ID: 7ECB). We introduced a positive charge on the surface of the enzyme and increased the binding rate to improve the PET-degrading activity. The binding rate constant of PET2-7M was (7.5 ± 3.0) × 10^8 s^{-1} μm^{-2} M^{-1}, which is 2.7 times higher than that of wild-type (WT) ((2.8 ± 1.6) × 10^8 s^{-1} μm^{-2} M^{-1}). PET2-7M (100 nM) produced 130 μM products, which was three times higher than that produced by PET2-WT (38 μM), from a 16 mg mL^{-1} PET film at pH 7.0 and 68 °C (WT at 60 °C) after 24 h of incubation. This improvement of activity was achieved by the improvement of electrostatic interaction between positively charged PET2 and electron-rich PET. However, the activity of PET2-7M remains insufficient for practical use.

The degradation of a solid polymer substrate catalyzed by an enzyme is a heterogeneous reaction at the liquid and solid interface, and not all of the bound enzymes can hydrolyze the substrate chain. Only the molecules that can form a productive complex generates reaction products. Therefore, the efficiency of the reaction can be represented by the number of bound molecules per unit time and the probability of forming a productive complex. In the case of crystalline chitin hydrolase, only 5% of the bound enzyme forms a productive complex.[34] The PET2 variant still has the potential to further increase the binding rate to the PET molecular chain by modifying the substrate-binding cleft.

In this study, additional mutations on PET2 WT were investigated using random and site-directed mutagenesis to find new possibilities and limitations of enzyme surface modification. Introduction of positive charges and hydrophilicity was also applied to the PET2 variant. In addition, to increase the substrate recognition ability, we modified the

https://doi.org/10.1021/acssuschemeng.5c01602
ACS Sustainable Chem. Eng. 2025, 13, 10404−10417

active site cleft based on a high-activity PETase variant. Furthermore, optimal conditions for enzyme production using *Komagataella phaffii* (*Pichia pastoris*) as a host and PET hydrolysis activity were tested using a fermenter scale. Finally, the degradation activities of the PET2 variant against PET fibers and blended fibers of PET, cotton, and PU were compared with those of LCC-ICCG.

2. EXPERIMENTAL SECTION

2.1. Homology Modeling of the PET2 WT Structure for Selection of Mutation Positions. A homology modeling structure of PET2 WT, structural preparation, docking analyses by 2-HE(MHET)$_3$, and predictions of disulfide bonds were performed using MOE v.2022.02 (Chemical Computing Group, Montreal, Canada). A homology modeling structure of PET2 WT was constructed using the crystal structure of IsPETase (PDB ID:6EQE) as a template.

2.2. Plasmid Construction and Enzyme Purification. The gene registered as an alkali-thermostable lipase, lipIAF5-219 (UniProt: C3RYL0), fused with a histidine-6 tag at the C-terminus, was synthesized. The gene was ligated into the pET28a plasmid using In-Fusion (TaKaRa Bio). SHuffle T7 Express Competent *E. coli* (Biolabs) were transformed with the plasmid and spread on an LB plate containing 25 μg mL^{-1} kanamycin. Colonies were harvested in 4 mL of LB medium after overnight incubation at 30 °C and inoculated into 30 mL of LB medium containing 25 μg mL^{-1} kanamycin. The flask was shaken at 220 rpm and 30 °C for 3 h. Next, 20 μL of 1 M isopropyl β-*d*-1-thiogalactopyranoside (IPTG) was added to the flask and incubated at 15 °C and 220 rpm for 16 h. The cells were harvested by centrifugation at 8000 rpm for 5 min.

Harvested cells were suspended in 50 mM 3-(N-morpholino) propanesulfonic acid (MOPS) buffer (pH 7.2) containing 500 mM sodium chloride at a concentration of 1 g mL^{-1}. The cells were suspended, disrupted using xTractor Buffer (TaKaRa Bio), and centrifuged at 13,000*g* for 10 min. The supernatant was loaded into 5 mL of TALON Metal Affinity Resin (TaKaRa Bio) equilibrated with 50 mM MOPS buffer (pH 7.2) containing 500 mM sodium chloride. The unbound fraction was washed with 5 mL of buffer containing 5 mM imidazole. The purified enzyme was eluted using a buffer containing 500 mM imidazole. The eluate was ultrafiltered using an Amicon Ultra Centrifugal Filter 10 kDa MWCO (Merck). The enzyme concentration was calculated using the TaKaRa Bradford Protein Assay Kit.

Genes encoding PET2 mutants with site-specific mutations were constructed by a polymerase chain reaction (PCR) using PrimeSTAR Max DNA Polymerase (TaKaRa Bio). Random mutations were introduced using the Diversify PCR Random Mutagenesis Kit (TaKaRa Bio) under the conditions of 7.2 mut kbp^{-1}. Primer pairs, including mutations, were used, and the products were ligated using In-Fusion (TaKaRa Bio), according to the manufacturer's instructions. The plasmids were transformed into SHuffle T7 Express Competent *E. coli* (Biolabs) and incubated at 37 °C for 1 h, followed by plating on LB agar plates containing 25 μg mL^{-1} kanamycin. A single colony was inoculated into 4 mL of LB medium and cultured overnight at 30 °C. The plasmid was purified from cells, and the sequence of the coding region was confirmed. The mutants were purified using the same procedure as that used for the WT.

2.3. Screening of Random Mutant Colonies Using Plates. Since random screening for mutations requires a high-throughput processing method, we employed a plate evaluation system using the tributyrin assay.[35] PET2, which has polyesterase activity, is also a lipase and can hydrolyze tributyrin. Furthermore, the addition of tributyrin to a normal LB agar plate makes the plate cloudy, and when tributyrin is degraded by the PET2 mutant, the plate becomes transparent (halo), which enables a rough estimation of the PET degradation activity. To prepare the agar plates, 30 mL of a 50% (v/v) tributyrin (FUJIFILM Wako Pure Chemicals) solution was prepared in sterile distilled water. 30 mL of 50 g L^{-1} arabic gum (SAN-EI YAKUHIN BOEKI) solution was prepared in distilled water, filtered through a 0.45 μm filter, and sterilized by UV irradiation for 1 min. Because the arabic gum solution was too viscous to pass through the 0.2 μm filter, a 50% (v/v) tributyrin solution and 50 g L^{-1} arabic gum solution were mixed 1:1 and sonicated using the BIORUPTOR2 sonicator (Sonic Bio). Arabic gum acts as an emulsifier for tributyrin. A total of 60 mL of tributyrin and arabic gum mixture was added to 1 L of sterilized molten LB agar medium and mixed. 20 mL of the mixture was placed in a Petri dish and solidified. *E. coli* was transformed using a plasmid library encoding the PET2 mutant gene, and colonies were formed on LB agar plates. The colonies were replicated on tributyrin-free and tributyrin-supplemented agar plates. After overnight incubation at 30 °C to confirm colony formation, tributyrin-supplemented agar plates were incubated overnight at 65 °C. To confirm whether the thermostability of the PET2 mutant had been improved, polyesterase activity was checked by incubating the tributyrin-supplemented agar plate at 65 °C. However, this temperature is usually higher than the incubation temperature of *E. coli*, making plasmid purification, sequencing analysis, and glycerol stock preparation difficult. So, from the tributyrin-free plates, colonies were obtained that corresponded to the colonies that formed halos on the tributyrin-supplemented agar plates, inoculated into 4 mL of LB medium, and incubated overnight at 30 °C. The plasmid was purified from cells, and the sequence of the coding region was confirmed. The mutants were purified using the same procedure as that used for the WT.

PET powder was used as a substrate to assess the mutant activity. Enzymatic reactions were performed using a ThermoMixer C (Eppendorf) with 0.5 mL of a reaction solution containing 10 μg mL^{-1} enzyme, 300 mM sodium phosphate buffer (pH 8.0), and 20 mg mL^{-1} PET powder at a reaction temperature of 60 °C for 24 h at a stirring speed of 1200 rpm. The degradation products of PET, TPA, mono-2-hydroxyethyl terephthalate (MHET), and bis(2-hydroxyethyl) terephthalate (BHET) were quantified at the end of the reaction.

2.4. Enzyme Surface Modification. Six single mutations (Y55S, A59R, S108R, L220K, T249K, and A264R) were introduced on the PET2-14M gene by PCR using the primer including the corresponding mutations, and mutant enzymes were prepared with the same procedure using *E. coli* as a host. PET powder was used as a substrate to assess mutant activity. Enzymatic reactions were performed using a ThermoMixer C (Eppendorf) with a 0.5 mL reaction solution containing 10 μg mL^{-1} enzyme, 300 mM sodium phosphate buffer (pH 8.0), and 20 mg mL^{-1} PET powder at a reaction temperature of 60 °C for 24 h at a stirring speed of 1200 rpm. The degradation products of PET, TPA, MHET, and BHET were quantified at the end of the reaction. The structures of PET2-14M and 14M-Y55S-A264R were predicted by the alphafold server,[36] and the surface charges of the mutants and IsPETase at pH 8.0 were estimated using the APBS Electrostatics plugin[37] in PyMOL.

2.5. T_m Measurement of PET2. *E. coli* SHuffle T7 (NEB) was transformed with plasmids encoding PET2-14M, 14M-Y55S, and 14M-A264R and spread on LB plates containing 50 μg mL^{-1} kanamycin after 1 h of incubation at 30 °C and 1000 rpm in Super Optimal broth with a catabolite repression (SOC) medium. Colonies were inoculated in 100 mL of super broth medium (2.5% tryptone, 1.5% yeast extract, and 0.5% NaCl) containing 25 μg mL^{-1} kanamycin and incubated overnight. 100 mL of the culture medium was added to 600 mL of the super broth medium containing 25 μg mL^{-1}; after 3 h of incubation at 30 °C and 130 rpm, 700 μL of 1 M IPTG was added, and it was further incubated at 16 °C and 130 rpm for 16 h. Cells were suspended in 50 mM sodium phosphate buffer, pH 7.0, containing 100 mM sodium chloride and sonicated for 20 min on ice. The supernatant was collected after centrifuging at 2000 g for 20 min and loaded onto Ni-NTA agarose (Qiagen). The resin was washed with 50 mM sodium phosphate buffer, pH 7.0, containing 100 mM sodium chloride, and the same buffer containing 50 mM imidazole. The enzymes were eluted using a buffer containing 100 mM imidazole and concentrated using a VIVA spin20 (30 kDa MWCO). The concentrated enzyme was injected into Superdex200 Increase and eluted with 20 mM sodium phosphate (pH 7.0), and the buffer was

https://doi.org/10.1021/acssuschemeng.5c01602
ACS Sustainable Chem. Eng. 2025, 13, 10404−10417

changed to 50 mM sodium phosphate pH 7.0 containing 100 mM sodium chloride.

Next, 400 μL of 20 μM enzyme was loaded into the quartz cell, and the change in the CD signal at 230 nm was measured from 20 to 110 °C by using a J-1500 CD spectrometer equipped with a Peltier thermostatic cell holder (JASCO). The melting temperature (T_m) of the enzyme was estimated by curve fitting of the temperature dependence of the signal at 230 nm using Denatured Protein Analysis software (JASCO).

2.6. Mutations around the Active Site. Six mutations (G134K-S136E-N200H-A227K-L228E-H229Y) were introduced into the PET2-14M gene by PCR using the primer, including the six mutations, and the PET2-14M-6Hot gene was constructed. The six mutation points of the PET2-14M-6Hot gene (K134, E136, H200, K227, E228, and Y229) were further replaced with the other 19 residues one by one. The enzymes were prepared using the same procedure using *E. coli* as a host, and the activities of the mutants against PET powder were compared. Enzymatic reactions were performed using a ThermoMixer C (Eppendorf) with a 0.5 mL reaction solution containing 10 μg mL^{-1} enzyme, 300 mM sodium phosphate buffer (pH 8.0), and 20 mg mL^{-1} PET powder at a reaction temperature of 60 °C for 24 h at a stirring speed of 1200 rpm. The degradation products of PET (TPA, MHET, and BHET) were quantified at the end of the reaction.

2.7. Enzyme Production by *K. phaffii*. The genes encoding the PET2 variants and LCC-ICCG, which have codons optimized for *K. phaffii*, were ligated into the AOX-Dasher GFP (ATUM) plasmid using In-Fusion (TaKaRa Bio) with primer pairs, following the manufacturer's instructions. The plasmid was transformed into *K. phaffii* (*P. pastoris* PPS-9011 (aox1Δ (Muts)) by electroporation, and the cells were cultured at 30 °C for 72 h on yeast extract, peptone, dextrose (YPD) plates containing 100 μg mL^{-1} Zeocin and 182 mg mL^{-1} D-sorbitol.

Screening of cultures for the copy number of genes in the obtained colonies was performed for the PET2 variants. YPD plates containing 182 mg mL^{-1} D-sorbitol at Zeocin concentrations ranging from 100 mg L^{-1} to 2000 mg L^{-1} were prepared, inoculated with colonies obtained by transformation, and incubated at 30 °C for 72 h. The copy number of genes in colonies grown on the plates at each concentration was quantified by quantitative polymerase chain reaction (qPCR) using a Thermal Cycler Dice Real Time System (TaKaRa Bio).

Fed-batch culture was performed using a BioLector XT (BECKMAN COULTER) microbioreactor to confirm the correlation between the copy number of genes and enzyme production. Colonies were cultured in test tubes containing 4 mL of buffered glycerol complex (BMGY) medium for 24 h with shaking. 40 μL of the culture medium was inoculated into 32-well plates containing 800 μL of the basal salt medium (BSM) containing 0.1 M 2-(N-morpholino) ethanesulfonic acid (MES) buffer and incubated with agitation at 1000 rpm while maintaining it at pH 5 with 10% ammonia−water and 60% concentration of O_2 aeration. After 16.5 h of incubation, 50 μL of 800 g L^{-1} glycerol was added, and the O_2 concentration of the aeration was changed to 80% for 1.5 h. After 18 h of incubation, dissolved oxygen (DO) was confirmed to be above 30%, and 50% methanol (v/v) was added at a flow rate of 1 μL h^{-1}. After 65 h of incubation, the culture was terminated by stopping agitation, aeration, addition of ammonia−water, and addition of methanol. Cell growth was assessed by measuring absorbance at 660 nm using a UV-1900i UV−vis spectrophotometer (Shimadzu) at the end of the culture. The culture medium was centrifuged at 8000*g* for 5 min at 4 °C, and the supernatant was collected. The amount of PET2 expression in the collected supernatant was evaluated by comparing the degradation activity of 4-nitrophenyl octanoate (pNO) with that of PET2-14M-6Hot as a standard. The supernatant was diluted in 1 × Rxn Buffer (50 mM HEPES, 2 mM $CaCl_2$−$2H_2O$, 0.5% (w/w) Triton X-100) and added to 96-well plates (50 μL each) and incubated at 30 °C. 50 μL of 2 mM pNO (Sigma-Aldrich) was added, and the degree of increase in 4-nitrophenol produced by the reaction was measured by the change in absorbance at 405 nm. MICROPLATE READER SH-9000 (CORONA ELECTRIC) was used for the measurement. Calibration curves were prepared by diluting purified PET2-14M-6Hot, whose concentration was known for protein quantification, with 1 × Rxn buffer in the concentration range of 0.5 to 5 mg L^{-1}. Protein quantification was performed using a TaKaRa Bradford Protein Assay Kit (TaKaRa Bio). PET2 expression in the culture was calculated by adding a dilution factor to the PET2 concentration obtained from the assay.

Colonies were inoculated into flasks containing 300 mL of BMGY medium and incubated at 30 °C for 30 h with shaking. Then, 35 mL of the resulting culture was inoculated into a jar fermenter (Biott) containing 350 mL of BSM medium and incubated at 30 °C and pH 5.0, with controlled aeration and agitation so that DO did not fall below 20%. The DO peak appeared when glycerol in the BSM medium was completely consumed, and glycerol feed was used as an indicator. The glycerol feed was stopped when the OD_{660} value of the yeast reached 200 (22 h of incubation), and the methanol feed was applied again, using the DO increase as an indicator. The incubation temperature was changed from 30 to 21−29 °C during the methanol feeding. Cultivation with a methanol feed was performed for 137 h. LCC-ICCG cells were cultured using the same procedure as that for the PET2 mutant.

2.8. Enzyme Purification from the Culture Medium of *K. phaffii*. After the *K. phaffii* culture was complete, the PET2 mutant and LCC-ICCG cultures were centrifuged, and the supernatant was collected. The supernatant was concentrated using an Amicon Ultra Centrifugal Filter (10 kDa MWCO; Merck); the buffer of the PET2 mutant concentrate was exchanged with 20 mM sodium acetate buffer (pH 5.0) and purified using SP Sepharose Fast Flow (Cytiva). The LCC-ICCG concentrate was exchanged with 10 mM Tris−HCl (pH 7.5) and purified using SP Sepharose High-Performance (Cytiva). The purified enzyme solution was concentrated using an Amicon Ultra Centrifugal Filter (10 kDa MWCO) and purified using Superdex 200 Increase (Cytiva). The purified enzyme solution was concentrated using an Amicon Ultra Centrifugal Filter, 10 kDa MWCO, and buffer-exchanged with PBS to obtain purified enzymes from the PET2 mutant and LCC-ICCG. The glycosylation states of purified PET2-14M-6Hot and LCC-ICCG were compared using a 10−20% gradient gel and 21 mA constant voltage for 70 min of SDS-PAGE.

2.9. Heat Resistance Measurement of PET2-21M. To confirm the thermostability of PET2-21M, PET2-21M was subjected to temperature loading, and then the activity assay using 4-nitrophenyl octanoate (pNO) as a substrate was performed to confirm residual activity. 80 μL of PET2-21M (concentration: 2.394 g L^{-1}) was dispensed into PCR tubes and incubated for 1 h using the Veriti 96-Well Thermal Cycler (Thermo Fisher SCIENTIFIC). The temperature conditions ranged from 55 to 90 °C, tested in 5 °C increments. After incubation, the enzyme solution was centrifuged at 5000*g* for 5 min at 4 °C, and the supernatant was collected. The recovered enzyme was diluted with 1 × Rxn buffer, added to 96-well plates in 50 μL aliquots, and then incubated at 30 °C. 2 mM pNO (Sigma-Aldrich) was added in a 50 μL volume, and the change in absorbance of 4-nitrophenol, the enzyme reaction product, was measured at 405 nm over 3 min with 5 s intervals. The activity of the enzyme stored at 4 °C without heat treatment was also measured, defined as 100%, and the residual activity was converted to a percentage of relative activity.

2.10. Large-Scale PET Degradation Test. Large-scale degradation studies of PET powder were performed using PET2-21M and LCC-ICCG. A reaction solution (300 mL) consisting of 100 mM sodium phosphate buffer (pH 8.0), enzyme concentrations of 2.5, 5.0, or 10 mg L^{-1}, and substrate concentrations of 20 and 40 g L^{-1} was prepared, and the reaction solution was placed in a jar fermenter (Biott). The crystallinity of the powder was 13%, and the average size of the particles was 100 μm. The enzymatic reaction was carried out for 24 h with the addition of 6 M NaOH at a controlled pH of 8.0, with agitation at 250 rpm. 6 M NaOH was added using a pump provided in the jar fermenter. Reaction temperatures were 60 °C for PET2-21M and 72 °C for LCC-ICCG. Reaction temperatures were maintained using an electrically heated jacket. PET degradation

https://doi.org/10.1021/acssuschemeng.5c01602
ACS Sustainable Chem. Eng. 2025, 13, 10404−10417

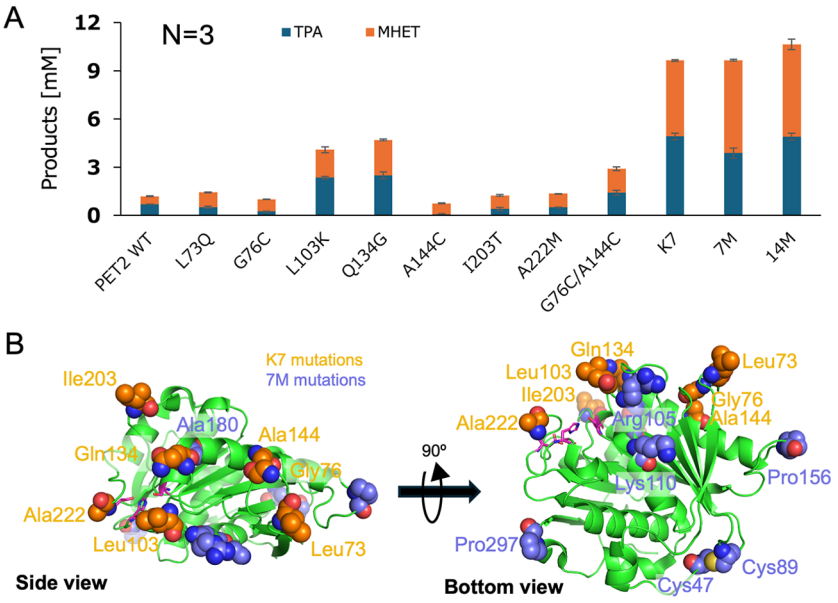

Figure 1. PET degrading activities of PET2 WT and variants and mutation positions of PET2-K7 and PET2-7M. (A) Effects of the single mutations on activities and activities of the combined variants PET2-K7, PET2-7M, and PET2-14M (combination of K7 and 7M). PET powders were degraded at 60 °C and pH 8.0 for 24 h. (B) Mutation positions of PET2-K7 and PET2-7M. The crystal structure of PET2-7 M (PDB ID: 7ECB) is shown in green cartoons, and the mutation positions of PET2-K7 and PET2-7M are shown as orange and blue spheres, respectively. The catalytic triad is indicated by a purple stick.

(TPA, MHET, and BHET) was determined over time by sampling every 2 h from 0 to 10 h until the end of the reaction.

2.11. PET Fiber Degradation. Degradation tests were performed on the PET fiber, PET/PU-blended fiber, and PET/cotton-blended fiber using PET2-14M-6Hot and LCC-ICCG. A 0.5 mL reaction solution consisting of 10 μg mL^{-1} enzyme, 100 mM sodium carbonate buffer (pH 9.2), and 20 mg mL^{-1} PET powder was prepared, and enzymatic reactions were performed at reaction temperatures of 50 °C, 60 °C, and 70 °C for 24 h at an agitation speed of 1200 rpm using a ThermoMixer C (Eppendorf). Since the pH cannot be controlled in this experiment, the formation of TPA due to PET degradation causes a decrease in pH, resulting in a decrease in the degradability of PET. Therefore, a sodium carbonate buffer (pH 9.2) was used to slightly increase the initial pH of the reaction to suppress the decrease in PET degradability due to the pH decrease. Sampling was performed every 2 h from 0 to 10 h, and the amount of PET degradation (TPA, MHET, and BHET) was quantified over time until the end of the reaction. The crystallinities of the PET fiber, PET/PU-blended fiber, and PET/cotton-blended fiber powders were 12%, 15%, and 16%, respectively. Their average sizes were 146, 134, and 78.0 μm, respectively.

2.12. Comparison of PET Fiber Degradation Activity at the 24 h Reaction End Point. Degradation tests were performed on the PET fiber, PET/PU-blended fiber, and PET/cotton-blended fiber using PET2-14M-6Hot and LCC-ICCG. A 0.5 mL reaction solution was prepared, consisting of 10 μg mL^{-1} and 50 μg mL^{-1} enzyme to determine whether changes in the amount of the enzyme cause changes in the amount of PET degradation, 100 mM sodium carbonate buffer (pH 9.2), and 20 mg mL^{-1} PET powder. Enzymatic reactions were performed at reaction temperatures ranging from 30 to 80 °C for 24 h, with an agitation speed of 1200 rpm using a ThermoMixer C (Eppendorf). The amount of PET degradation (TPA, MHET, and BHET) was quantified at the end of the 24 h reaction. The same PET fiber, PET/cotton-blended fiber, and PET/PU-blended fiber used in the PET fiber degradation were utilized.

2.13. PET Degradation Activity Measurement. PET powder was kindly gifted by TOYO SEIKAN Co. Ltd. The PET fiber, PET/cotton-blended fiber (PET content 65%), and PET/PU-blended fiber (PET content 85%) were purchased from TEIJIN FRONTIER Co., Ltd., SHIKIBO Ltd., and Shikisensha CO., Ltd., respectively. The PET bottles, PET fiber, PET/PU-blended fiber, and PET/cotton-blended fiber were melted, pelletized, and then ground into a powder by using a milling device. The degradation products TPA, MHET, and BHET were quantified using HPLC. After the enzymatic reaction, the solution was centrifuged, and the supernatant was collected, filtered through a 0.2 μm filter, and diluted with dimethyl sulfoxide as appropriate. The supernatant was analyzed using an LC-2060C 3D liquid chromatograph (Shimadzu). Analysis was performed under the following conditions: the column was Discovery HS C18 15 cm × 4.6 mm 5 μm (Supelco) connected to a guard column of Discovery HS C18, Kit 2 cm × 4 mm, 5 μm (Supelco); column oven temperature, 25 °C; mobile phase, 0.1% formic acid and 20% acetonitrile (v/v); flow rate, 0.8 mL min^{-1}; detection wavelength, 240 nm; analysis time, 20 min; and sample applique volume, 10 μL. Calibration curves were prepared using commercially available TPA (FUJIFILM Wako Pure Chemicals), MHET (Amatek Chemical), and BHET (Tokyo Chemical Industry) in the range of 0−30 mg L^{-1}. The molar concentrations were calculated by dividing the measured TPA, MHET, and BHET concentrations by the molecular weights of TPA, MHET, and BHET, respectively.

3. RESULTS

3.1. Screening and Combination of Single Mutations. To find new mutations for improving the activity of PET2, we applied random mutations to PET2 WT and analyzed 3129 colonies using activity screening with tributyrin agar plates. The colonies which had the gene coding for PET2 L73Q and I203T showed a larger halo than PET2 WT and higher PET degradation activity than WT (Figure 1A). Furthermore, L103K, Q134G, and A222M from the library of site-saturated mutants at the substrate-binding cleft, showing higher activity than WT, were accepted. We also introduced the G76C and A144C mutations because disulfide bond formation was expected from the predicted structure. We summarized the PET degradation activities of the seven variants and PET2 WT in Figure 1A. L103K and Q134G mutations showed 3.4 and 3.9 times higher total products (4.1 and 4.7 mM, respectively) than the WT (1.2 mM) against 21 mg mL^{-1} PET powder in

https://doi.org/10.1021/acssuschemeng.5c01602
ACS Sustainable Chem. Eng. 2025, 13, 10404−10417

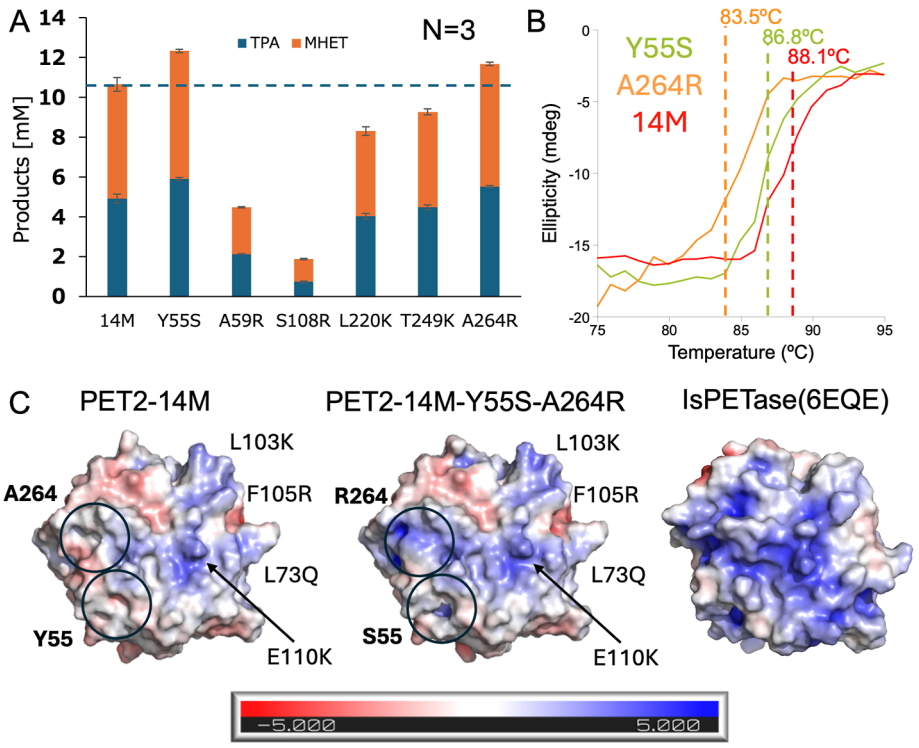

Figure 2. Effects of positive-charge mutations. (A) The effect of single mutations on PET2-14M. Activities against PET powder at 60 °C and pH 8.0 for 24 h were compared. (B) T_m determination from the CD signal. The T_m value of PET2-14M was 88.1 °C and those of PET2-14M-Y55S and PET2-14M-A264R were 86.8 and 83.5 °C, respectively. (C) Surface charges of PET2-14M, PET2-14M-Y55S-A264R, and IsPETase (PDB ID: 6EQE) at pH 8.0. Charges were estimated using the ABPS program and visualized using PyMOL.

300 mM sodium phosphate buffer pH 8.0 at 60 °C for 24 h. The L73Q, I203T, and A222M mutations were weaker than the other two, but their activities were 1.2, 1.3, and 1.4 times higher than that of the WT. The cysteine mutants G76C and A144C showed similar or lower activity compared with the WT, respectively, but the double mutant G76C/A144C exhibited 2.9 times higher activity than the WT. These results suggest that the C76 and C144 formed a disulfide bond, and the stability of the enzyme was increased. The combined mutant PET2-K7 (L73Q-G76C-L103K-Q134G-A144C-I203T-A222M) showed 8.1 times higher activity than PET2 WT and was almost similar to PET2-7M (R47C-G89C-F105R-E110K-S156P-G180A-T297P) previously reported.[33] The combined mutant PET2-14M (R47C-L73Q-G76C-G89C-L103K-F105R-E110K-Q134G-A144C-S156P-G180A-I203T-A222M-T297P) showed slightly higher activity than PET2-7M and 8.9-times higher activity than the WT. The mutated positions are shown in Figure 1B. Mutations were spread over the surface. Importantly, the bottom side of PET2 in Figure 1B, which is expected to interact with the PET surface, was positively charged by a combination of mutations (L103K-F105R-E110K).

3.2. Enzyme Surface Modification. We also tested whether the binding rate on PET and the degradation activity could be improved by introducing a positive charge on the enzyme surface. To further modify the surface charge, we screened for five arginine/lysine mutations and one serine mutation on the positively charged surface of PET2-14M. The Tyr55, Ala59, Ser108, Leu220, Thr249, and Ala264 residues, whose carbonyl group on the main chain forms a negatively charged patch and whose side chain is oriented toward the solvent, were chosen as mutation targets. PET2-14M produced 4.9 mM TPA and 5.7 mM MHET from PET powder, and additional Y55S and A264R mutations showed 1.2 and 1.1 times higher concentration of the sum of the products, respectively (Figure 2A). Other positively charged mutations decreased the activity of PET2-14M. Then, effects of Y55S and A264R on the stability of PET2-14M were determined using T_m measurements based on the changes in the CD spectrum (Figure 2B). PET2-14M showed a T_m of 88.1 °C in 50 mM sodium phosphate (pH 7.0) containing 100 mM sodium chloride. Under the same conditions, the T_m values of Y55S and A264R mutants were 86.8 and 83.5 °C, respectively. These values were larger than those of PET2 WT (T_m = 68.0 °C) and PET2-7M (T_m = 75.7 °C).[33] These results suggest that G76C and A144C of the K7 mutations formed a disulfide bond. Y55S and A264R decreased the thermal stability of PET2-14M but did not significantly affect the degradation reaction at 60 °C. To consider the reasons for the improvement in activity, charges on the enzyme surface were calculated using the APBS Electrostatics plugin in PyMOL (Figure 2C). The A264R mutation clearly extended the positively charged patch at pH 8.0, whereas the Y55S mutation removed neutral protrusions and increased the positively charged surface area. The modified surface of PET2-14M-Y55S-A264R was closer to that of the positively biased IsPETase than PET2-14M.

3.3. Mutations around the Active Site. The catalytic triad of PET2-14M was Ser175, Asp221, and His253. Around the catalytic residues, Tyr102, Met176, Trp199, Ile223, Trp254, which are the same residues as HotPETase, and Gly134, Ser136, and Asn200 form the active-site cleft. Ala227, Leu228, and His229 interact with Trp199 and support the formation of the active-site cleft. Then, the active-site residues were further mutated using HotPETase as a reference (Figure

https://doi.org/10.1021/acssuschemeng.5c01602
ACS Sustainable Chem. Eng. 2025, 13, 10404−10417

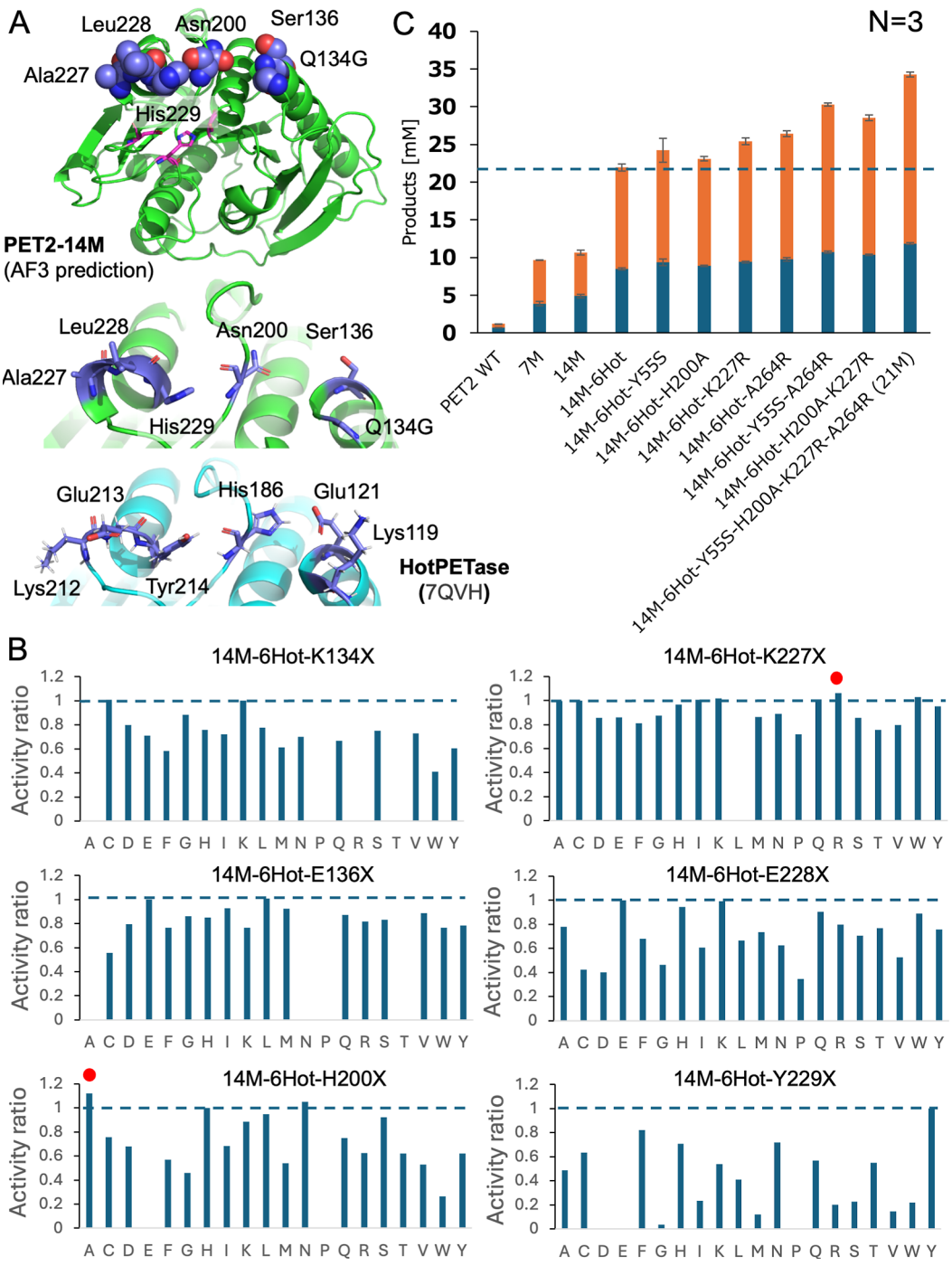

Figure 3. Substrate binding site modifications. (A) Target residues of PET2-14M are shown in blue spheres, and the catalytic triad is shown in magenta (top). Close-up view of the target residues of PET2-14M. The responsible mutations in HotPETase are shown in blue (bottom). (B) Mutation optimization of PET2-14M-6Hot. The accepted mutations that improved the activity are indicated by red marks. (C) Comparison of the activities of the combined variants against PET powder at pH 8.0 and at 60 °C for 24 h.

3A). Six residues (Lys119-Glu121-His186-Lys212-Glu213-Tyr214) of the HotPETase, which make the substrate binding cleft and are located on a structure similar to that of PET2, were introduced into PET2-14M at the corresponding positions (Gly134-Ser136-Asn200-Ala227-Leu228-His229). As a result, a new variant, PET2-14M-6Hot (PET2-R47C-L73Q-G76C-G89C-L103K-F105R-E110K-Q134K-S136E-A144C-S156P-G180A-N200H-I203T-A227K-L228E-H229Y-A222M-T297P) was prepared. Note that the Q134G mutation was already introduced in PET2-14M and was overridden by the Q134K mutation. Then, the 6 mutated sites (Q134K-S136E-N200H-A227K-L228E-H229Y) were further optimized one by one, by checking the activities of site-saturated mutants (Figure 3B). Some mutations (for example, K134P) completely lost their activities, but H200A, H200N, and K227R showed higher activity than that of the template, PET2-14M-6Hot.

PET2-14M-6Hot produced 21.9 mM products from PET powder, which was 2.1 times higher than that of PET2-14M (Figure 3C). Next, the effects of Y55S, H200A, K227R, and

https://doi.org/10.1021/acssuschemeng.5c01602
ACS Sustainable Chem. Eng. 2025, 13, 10404−10417

A264R mutations in PET2-14M-6Hot were compared one by one, by measuring their PET powder degradation activities. All of them showed better activity than the template, and some combined mutations were further tested. The combination of Y55S-A264R and H200A-K227R increased the activity of PET2-14M-6Hot by 1.4- and 1.3-fold, respectively. Furthermore, PET2-14M-6Hot-Y55S-H200A-K227R-A264R (PET2-21M) had 1.6 times higher activity than PET2-14M-6Hot. Note that we named this variant PET2-21M because it contains 21 mutations (R47C-Y55S-L73Q-G76C-G89C-L103K-F105R-E110K-Q134K-S136E-A144C-S156P-G180A-N200A-I203T-A227R-L228E-H229Y-A222M-A264R-T297P) compared with PET2 WT (Figure 4). PET2-21M produced

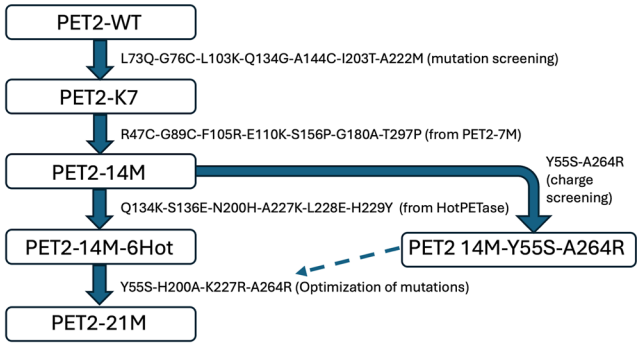

Figure 4. Flowchart of the PET2 variants' development.

11.6 mM TPA and 22.4 mM MHET from 21 mg mL^{-1} PET powder in 300 mM sodium phosphate buffer (pH 8.0) at 60 °C for 24 h. These concentrations were 17 and 44.8 times higher than those of PET2-WT, respectively. The total product concentration of PET2-21M was 28.6 times higher than that of PET2-WT.

3.4. Enzyme Production by *K. phaffii*. To produce the enzyme for large-scale PET degradation experiments, we constructed a PET2 enzyme production system using the methanol-utilizing yeast *K. phaffii* as the host. In *E. coli*, full-length proteins, including original signal sequences, were expressed. However, in yeast, we swapped the original signal sequence with that of human serum albumin (HSA) and deleted the N-terminal 15 residues of PET2 (Figure 5A). The *K. phaffii*, which has three copies of the expression cassette in the genome, showed the best growth and PET2 production in the medium, and used for the optimization of cultivation conditions to produce the enzyme (Figure S1).

The enzyme production was compared at different temperatures between 21 and 29 °C using PET2-14M-6Hot as the test enzyme (Figure 5B). In this temperature range, growths of *K. phaffii* with 4% glycerol as the carbon source were not different in the BSM medium. After growth in glycerol (approximately 22 h), MeOH was added to initiate the induction of PET2. MeOH feeding was linked to an increase in the OD_{660}. Incubation at 23 and 25 °C resulted in higher MeOH consumption and an increase of OD_{660}. Productions of PET2 at 23 and 25 °C were better than those at other temperatures. Finally, 691 mg L^{-1} PET2-14M-6Hot was produced after 137 h of incubation at 23 °C. PET2-14M-6Hot was not modified with sugar chains by *K. phaffii* and was detected as a clear single band in SDS-PAGE (Figure S2A). This was due to the deletion of the consensus sequence for *N*-glycosylation (Asn-X-Ser) by the N200H mutation.[38] PET2-21M and LCC-ICCG were produced in the same way, and LCC-ICCG was modified with the sugar chain (Figure S2B) as previously reported.[39]

3.5. Large-Scale PET Degradation. PET powder was degraded by *K. phaffii*-produced PET2-21M on a 300 mL scale using a fermenter. First, the activity of PET2-21M and LCC-ICCG was compared at a substrate concentration of 20 g L^{-1}. This is the same substrate concentration used in the activity screening of the mutants. The thermostability of PET2-21M was evaluated from the remaining activity after heat treatment (Figure S3), and the reaction temperature for PET2-21M was set as 60 °C. 95% of 20 g L^{-1} PET was degraded by 5 mg L^{-1} PET2-21M after 24 h at 60 °C and pH 8.0 (Figure 6A). LCC-ICCG showed 91% degradation of 20 g L^{-1} PET after 10 h of incubation at 72 °C. In contrast, under the condition of 20 g L^{-1} PET and 2.5 mg L^{-1} enzyme (Figure 6B), PET2-21M degraded 50% of PET (53 mM total products) after 24 h of incubation, but LCC-ICCG degraded only 26% of PET (27 mM total products).

With twice the higher concentrations of PET (40 g L^{-1}) and enzyme (10 mg L^{-1}), LCC-ICCG degraded 95% of PET (198 mM total products) after 24 h of incubation at 72 °C, and PET2-21M showed 79% degradation (164 mM total products) at 60 °C after the same incubation time (Figure 6C). Furthermore, under the same PET/enzyme ratio conditions, a higher concentration of PET (40 g L^{-1}) was degraded using 5 mg L^{-1} enzyme. PET2-21M degraded 44% of PET (93 mM total products) after 24 h of incubation, but LCC-ICCG degraded only 29% of PET (60 mM total products) (Figure 6D).

3.6. PET Fiber Degradation. To assess the applicability of PET2-14M-6Hot and LCC-ICCG to the degradation of PET fibers, which are unused waste materials, their activities against three types of fibers were compared. Given that the products of PET2-14M-6Hot and LCC-ICCG from the three fibers were TPA and MHET, it was indicated that the other materials blended in did not decompose (Figure S4). After centrifugation, white particles remained in the tubes (data not shown). The activity of LCC-ICCG against pure PET fibers increased as the reaction temperature increased from 50 to 70 °C (Figure 7A). In contrast, PET2-14M-6Hot showed the best activity at 60 °C, and the product concentration did not increase after 2 h of incubation at 70 °C. Importantly, the highest total products (75.7 mM) were obtained by PET2-14M-6Hot at 60 °C. This value was 1.4 times higher than that of LCC-ICCG at 70 °C. The results for the PET/cotton-blended fibers were similar to those for the pure PET fibers (Figure 7B). PET2-14M-6Hot produced 62.8 mM total products at 60 °C, and LCC-ICCG produced 46.7 mM total products at 70 °C. Interestingly, the blended PET and PU fibers were not degraded at high temperatures (60 and 70 °C) but degraded at 50 °C for both PET2-14M-6Hot and LCC-ICCG (Figure 7C). Total product concentrations increased linearly with incubation time, PET2-14M-6Hot produced 19.2 mM total products at 50 °C, and LCC-ICCG produced 8.2 mM total products after 24 h of incubation. The temperature dependencies of PET and blended fiber degradation by PET2-14M-6Hot and LCC-ICCG were confirmed with more wide range (Figure S5).

4. DISCUSSION

Using a different approach from PET2-7M,[33] we found seven new mutations which improved the activity of PET2 WT. The

https://doi.org/10.1021/acssuschemeng.5c01602
ACS Sustainable Chem. Eng. 2025, 13, 10404−10417

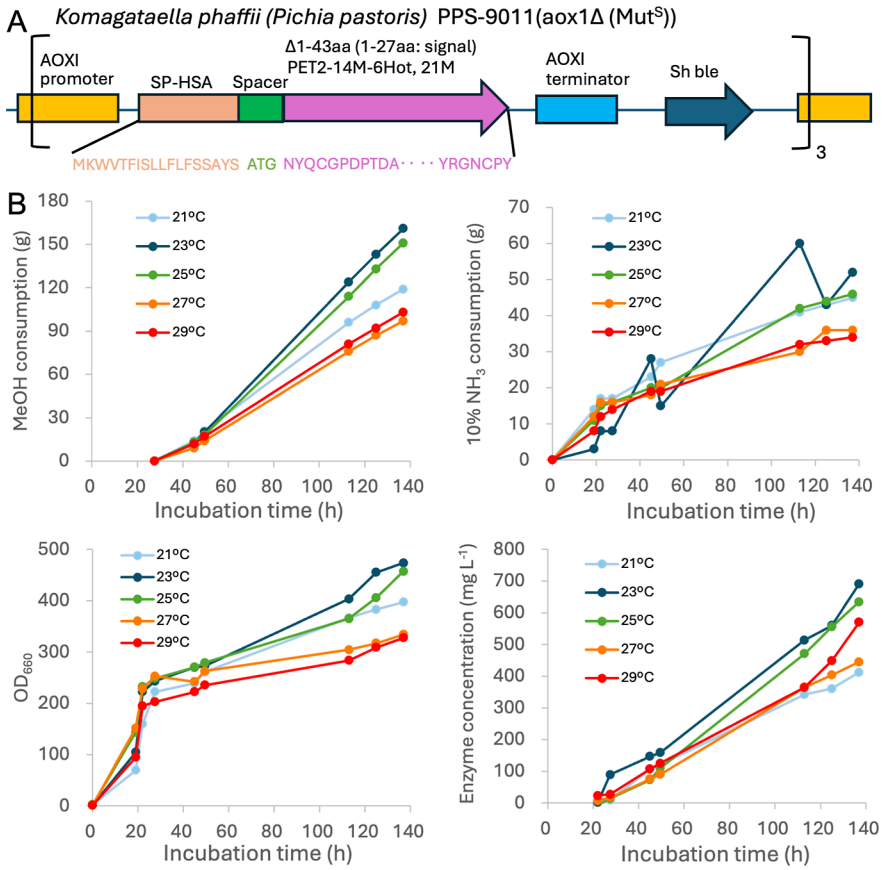

Figure 5. Expression cassette and optimization of *K. phaffii* cultivation. (A) Gene composition for PET2 variant expression. N-terminal 43 residues (1−27 residues correspond to the original signal sequence) were removed, and the HSA signal peptide was connected via a spacer sequence. (B) Temperature dependence of PET2-14M-6Hot production by *K. phaffii*.

combined mutant PET2-K7 showed activity similar to that of PET2-7M, and the activity of the integrated mutant PET2-14M was slightly improved (Figure 1A). The L103K mutation adds a positive charge to the PET interacting surface of PET2 (Figure 1B), and this mechanism is the same as that of the F105R-E110K mutations in PET2-7M, which form the IsPETase-like enzyme surface.[40] In PET2-7M, the binding rate constant increased 2.7-fold and the activity increased 3-fold due to the introduction of positive charges on the enzyme surface.[33] This indicates that the binding rate was the rate-limiting step in the PET degradation reaction in PET2. To identify another mutation that could expand the positively charged area on the surface, we mutated residues that could mask the negative charges on the surface. The A264R mutation masked the negative charge and increased the positively charged surface area (Figure 2C). The other four positions did not increase the activity, although almost all surfaces were positively charged by these mutations. Therefore, the rate-limiting step of the PET degradation reaction is no longer binding, and it was thought that there would be no effect of further activity improvement by positive charges.

The side chain of His186 of HotPETase forms a hydrogen bond with the main chain carbonyl of Ser202, which stabilizes the loop region and fixes the orientation of Trp185, making it suitable for PET chain binding.[27] In contrast, PET2 has a one-amino-acid longer loop with 200 to 206 residues, and His200 cannot form a stable hydrogen bond like HotPETase. Therefore, the H200A mutation was introduced in PET2-21M. Ala has a small hydrophobic side chain, and Ala200 is expected to tune the orientation of Trp199, which is a highly conserved residue in PET hydrolases.[41] This tryptophan residue is important for the binding and acylation of the PET chain at the active site,[42] the release of product,[43] and the entire reaction cycle.[44] In the case of PET2, the optimal arrangement of the Trp199 side chain angle increased PET hydrolysis activity.[45] H229T-F233 M mutations changed the secondary structure of the loop formed by residues Asn200 to Phe206 of PET2-7M and modified the C−C$_\alpha$−C$_\beta$−C$_\gamma$ dihedral angle (χ_{1C}) of Trp199 from + 65.7° to + 59.2°. Asn200 formed a hydrogen bond with Gln183 and locked the loop structure of PET2-7M (PDB ID: 7ECB) (Figure S6). Therefore, N/H200A mutations would free the loop and modify the chi1 angle of Trp199 to increase PET hydrolysis activity. Another difference is Lys212 of HotPETase and the corresponding Arg227 of PET2-21M. Lys212 of HotPETase forms a hydrogen bond with Asp283. PET2-21M (and PET2-7M) also has Glu301 at the corresponding position, but this residue forms a hydrogen bond network with Arg303, Ser231, and Asn235 in the crystal structure of PET2-7M (Figure S7). Therefore, even if the R227K mutation is introduced, hydrogen bond formation between Lys227 and Glu301 would be difficult. Instead, Arg227 formed a hydrogen bond with Glu228 in the predicted structure of PET2-21M.

Since we could not obtain sufficient enzyme yield for use in large-scale PET degradation experiments using *E. coli*, we constructed an expression system using *K. phaffii* as the host. IsPETase and Fast-PETase can be produced by *K. phaffii* using native signal peptide[46] and α-factor,[47,48] but PET2 production

https://doi.org/10.1021/acssuschemeng.5c01602
ACS Sustainable Chem. Eng. 2025, 13, 10404−10417

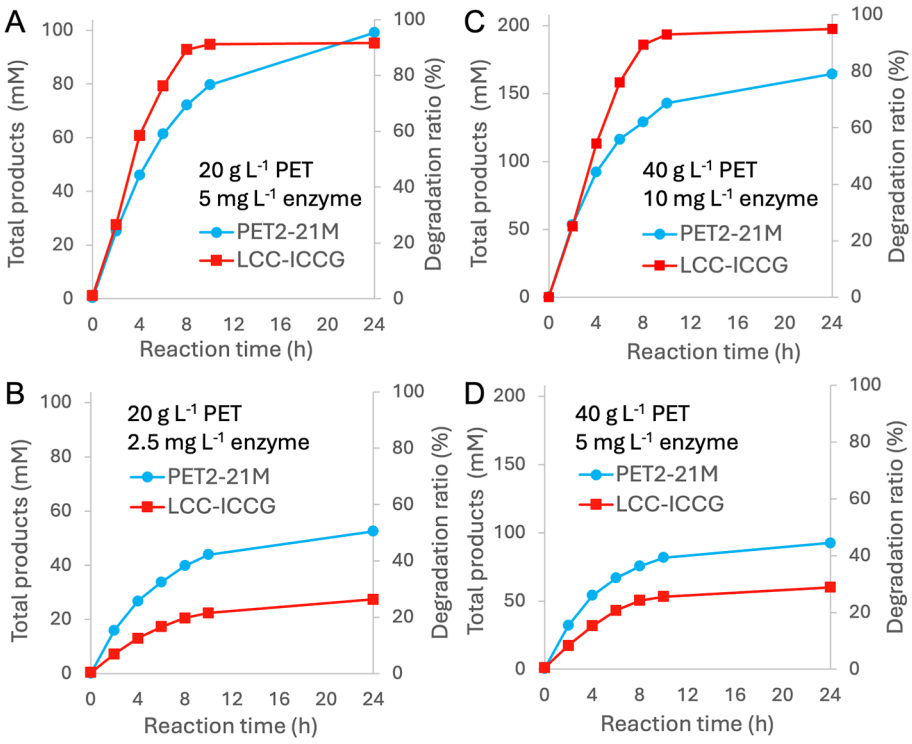

Figure 6. Large-scale degradation of PET powder. (A) Degradation of 20 g L^{-1} PET powder with 5 mg L^{-1} enzyme. (B) Degradation of 20 g L^{-1} PET powder with 2.5 mg L^{-1} enzyme. (C) Degradation of 40 g L^{-1} PET powder with 10 mg L^{-1} enzyme. (D) Degradation of 40 g L^{-1} PET powder with 5 mg L^{-1} enzyme. The reaction pH was maintained at 8.0, by adding sodium hydroxide. PET2-21M was incubated at 60 °C, and LCC-ICCG was incubated at 72 °C.

by *K. phaffii* was not observed with the native signal sequence of PET2 or α-factor (data not shown). Therefore, we directly connected PET2 to the signal peptide of HSA and removed the N-terminal residues of PET2 (28−43 residues, numbering including the signal sequence), which were not modeled in the X-ray crystal structure.[33] Production of PET2 was best by the colony containing three copies of the expression cassette due to the optimal balance between enzyme production and growth. Shu et al. reported that the two copies of the expression cassette have been good to produce serine protease SPTK using *K. phaffii*, which has a similar catalytic mechanism to PET hydrolase.[49] The highest enzyme production efficiency was achieved at 23 °C. This is slightly lower than the usual temperature of *K. phaffii* growth and production of enzymes like LCC-ICCG[39] (30 °C). Given that the rate of methanol consumption and the rate of increase in OD_{660} at 23 and 25 °C are higher than at 29 °C, this may be due to the increased efficiency of methanol metabolism due to the increased dissolved oxygen content resulting from the lower temperature. The productivity of PET-14M-6Hot in *K. phaffii* is almost the same as that of *Bacillus subtilis* produced BhrPETase (0.66 g L^{-1}).[50] However, the productivity of PET-14M-6Hot is not as high as that of FastPETase using *K. phaffii* (3.0 g L^{-1})[48] or 4Mz (3.1 g L^{-1})[51] and VNp6-FastPETase (2.2 g L^{-1})[52] using *E. coli*, so further improvements are needed.

In a large-scale PET degradation experiment, 0.25 mg g-PET^{-1} LCC-ICCG decomposed 95% of 20 g L^{-1} PET at 72 °C after 10 h, with lower enzyme loading than Tournier et al.[22] (200 g L^{-1} PET with 1 mg-enzyme g-PET^{-1} at 72 °C) and Arnal et al.[29] (165 g L^{-1} PET with 1 mg-enzyme g-PET^{-1} at 68 °C). PET2-21M showed 100% degradation at 60 °C after 24 h with the same substrate and enzyme concentrations (Figure 6A). At higher concentrations of PET and enzyme, LCC-ICCG showed a similar curve of total product concentrations against incubation time, but the activity of PET2-21M decreased after 6 h of incubation, and the degradation was 79% at 24 h (Figure 6C). This decrease in activity might be due to product inhibition by MHET, as observed for TfCut2.[53] LCC-ICCG completely converted MHET to TPA after 24 h of incubation at 72 °C, but PET2-21M retained 63 mM MHET at the same incubation time at 60 °C (Figure S8). Under lower enzyme loading conditions (0.125 mg of enzyme/g of PET), PET2-21M showed better activity than LCC-ICCG (Figure 6B and D). The degradation of 20 g L^{-1} PET with 2.5 mg L^{-1} PET2-21M and 40 g L^{-1} PET with 5 mg L^{-1} PET2-21M showed 50% and 44% degradation after 24 h of incubation, respectively. These values are nearly half of the 0.25 mg of enzyme g-PET^{-1} loading conditions. However, LCC-ICCG degraded only 26% and 29% of PET under these conditions, respectively. These disparities may be attributable to variations in the reaction temperature. LCC-ICCG reacted at 72 °C, which is higher than the glass transition temperature (T_g) of PET. Cui et al. reported an increase in crystallinity during PET degradation at 72 °C with LCC-ICCG.[28] They also showed that the upper limit for the decomposition ratio of LCC-ICCG at 72 °C is 92.5% but that 97.7% decomposition is possible at 65 °C. Therefore, at 72 °C, degradation and crystallization of PET would compete. In this case, given the relatively low hydrolysis activity of PET hydrolase in the crystalline region of PET, it can be concluded that in order to achieve maximum degradation efficiency, it is necessary to accelerate the degradation of PET to prevent it from lagging behind the rate of crystallization. Consequently, the enzyme/substrate

https://doi.org/10.1021/acssuschemeng.5c01602
ACS Sustainable Chem. Eng. 2025, 13, 10404−10417

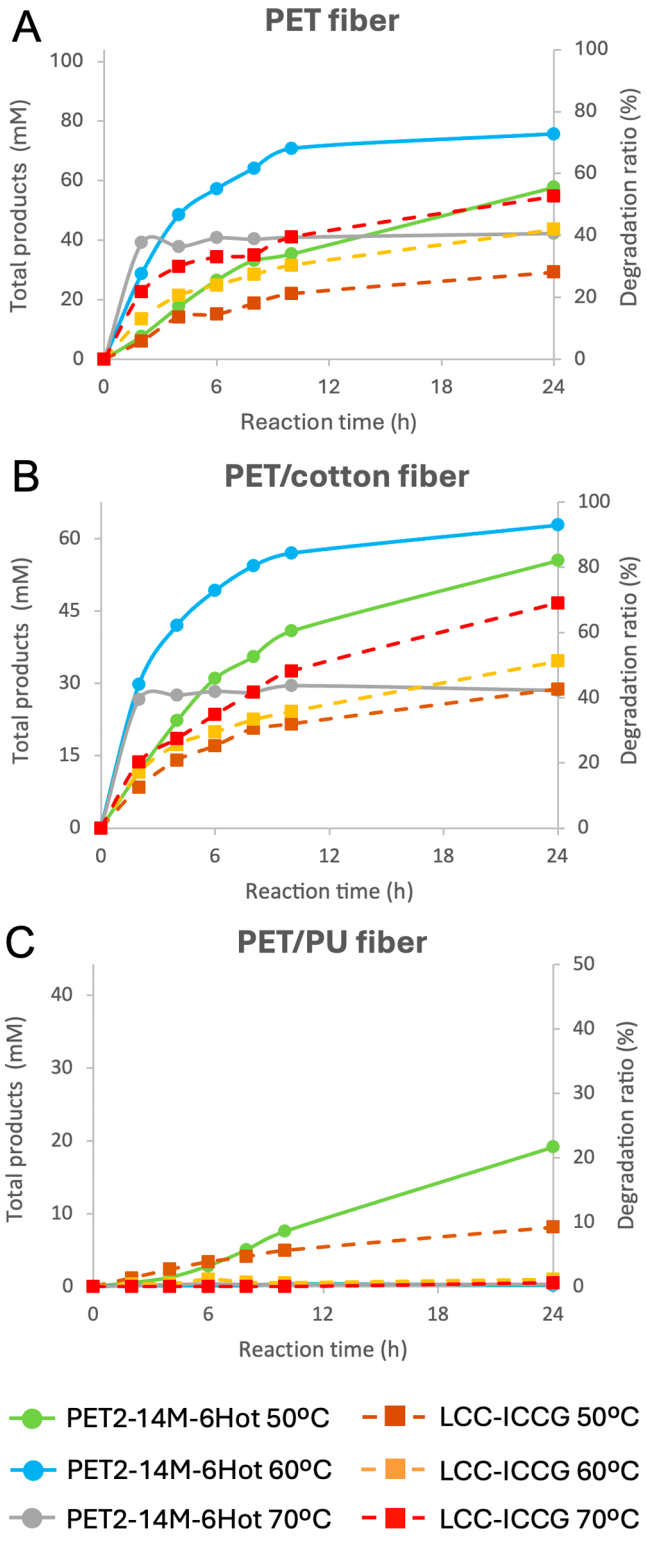

Figure 7. Degradation of pure and blended PET fibers. (A) Degradation of the pure PET fibers. (B) Degradation of PET/cotton-blended fibers. (C) Degradation of PET/PU-blended fibers. The substrates (20 g L^{-1}) were degraded by 10 mg L^{-1} enzymes under all conditions.

ratio is an important factor for the LCC-ICCG reaction at 72 °C.

One method is to increase the degradation activity of the enzyme and quickly degrade PET before crystallization with high enzyme loading. This is the approach taken with LCC-A2.[23] At an enzyme concentration of 3 mg g-PET^{-1}, 90% degradation occurs after 3.3 h at a high temperature of 78 °C. Another method is to lower the reaction temperature and reduce the rate of PET recrystallization, which allows the PET to be completely degraded, even if the enzyme concentration is lowered and the reaction time is increased. In fact, Arnal et al. achieved 98% degradation of 165 g kg^{-1} of PET with 1 mg g-PET^{-1} LCC-ICCG at 68 °C for 24 h.[29] In our case, PET2-21M completely degraded 20 g kg^{-1} PET with 0.25 mg g-PET^{-1} after 24 h at 60 °C. When the enzyme concentration was halved in PET2-21M, the product concentration was also halved, but when the enzyme concentration was halved in LCC-ICCG, the product concentration was reduced to one-fourth at 72 °C. From the point of view of robustness and completeness of PET degradation, the degradation reaction at lower than 70 °C is a good option. In addition, the cost of heating the reaction mixture is reduced if a PET hydrolase can degrade PET at a lower temperature. To avoid wasting the energy used for decrystallization by grinding and to increase the maximum degradation ratio, it is considered important to degrade rapidly at a temperature of 70 °C or less[29] such as TurboPETase, which degraded 200 g kg^{-1} PcPET with 2 mg g-PET^{-1} at 65 °C for 8 h.[28]

The degradation ability of PET fibers is also an important factor in the evaluation of PET hydrolases for PET recycling. Degradation by PET2-14M-6Hot at 60 °C showed better performance than degradation by LCC-ICCG at 70 °C against the PET fiber and PET/cotton-blended fiber (Figure 7A,B). The precise mechanism underlying PET2-14M-6Hot's enhanced capacity for degrading PET fibers remains to be elucidated. The reason for the activity difference does not come from the difference in crystallinity, because the fibers of PET (12−16%) were similar to those of PET from the bottle (13%). Pfaff et al. examined the relationship between activity and average molecular mass of PET and found that LCC-ICCG shows better performance against short PET chains than long PET chains.[54] They also reported that the weight-average molecular weight (M_w) of the postconsumer PET bottle was 32.3 kDa. In addition, Farah et al. reported that commercially available 14 PET-fibers have a Mw ranging from 28.6 to 66.5 kDa (only Trevira 350, labeled as A4 fiber, has a lower M_w than the PET bottle).[55] Therefore, PET2 variants may have the ability to degrade not only a short PET chain but also a long one. Interestingly, the pure PET fiber and blended PET/cotton fiber exhibited similar degradation patterns (Figure 7A,B). These results suggest that the PET and cotton fibers exist separately and do not affect each other in PET/cotton-blended fibers. This shows the advantage of the higher substrate specificity of enzymes over that of low-molecular-weight catalysts. In contrast, the blended PET/PU fibers exhibited different degradation patterns and temperature dependence (Figure 7C). Both PET2-14M-6Hot and LCC-ICCG showed linear and highest activities at 50 °C. At 60 and 70 °C, neither enzyme produced any products, although the optimum temperatures for PET hydrolysis by PET2-14M-6Hot and LCC-ICCG were 60 and 70 °C, respectively. In fact, more decomposition products were detected in the reaction at 30 °C using both enzymes than in the reaction at 60 °C (Figure S5). The T_g of PU is approximately 55 °C,[56] and a small transition was observed at approximately 66 °C in the differential scanning calorimetry (DSC) measurements of the PET/PU-blended fiber used in the present study (Figure S9). Therefore,

https://doi.org/10.1021/acssuschemeng.5c01602
ACS Sustainable Chem. Eng. 2025, 13, 10404−10417

during the reaction above 60 °C, polymer rearrangement may occur and the accessible PET surface is reduced. When solid polymer substrates are degraded, it is necessary to consider the structural changes in the substrate that depend on the reaction temperature. Although detailed mechanisms need to be elucidated in future studies, our results demonstrate that PET2 variants can be candidates for PET fiber recycling in the middle-temperature range. It was also pointed out that the properties of PET in the fiber form, which represents one of the most widely used forms of PET, may be different from those of PET in the bottle form. In particular, the need to develop new enzymes that work at low temperatures with high substrate specificity was emphasized.

5. CONCLUSIONS

By finding new mutations that improve the activity of PET2, integrating PET2-7M and optimizing the amino acids near the active site with reference to HotPETase, we successfully created PET2-14M-6Hot and PET2-21M. We developed an enzyme expression system using yeast and optimized the culture conditions, and 691 mg L^{-1} PET2-14M-6Hot was produced after 137 h of incubation at 23 °C. PET2-21M showed best activity at 60 °C, and 20 g L^{-1} PET powder was completely degraded in 24 h by 5 mg L^{-1} enzyme. Powdered PET fiber and PET/cotton-blended fiber were better degraded by PET2-14M-6Hot at 60 °C than LCC-ICCG at 70 °C. Powder of PET/PU-blended fiber was only degraded at 50 °C by PET2-14M-6Hot and LCC-ICCG. To minimize the impact of other components in blended fiber and PET recrystallization, enzymes that work efficiently at lower than 60 °C are expected to be highly beneficial.

■ ASSOCIATED CONTENT

Supporting Information

The Supporting Information is available free of charge at https://pubs.acs.org/doi/10.1021/acssuschemeng.5c01602.

> Effect of copy number of PET2 gene; SDS-PAGE images of enzymes; thermostability analysis of PET2-21M; chromatograms of products from PET and blended fibers; temperature dependences of degradations of PET and blended fibers; hydrogen bonding in PET-7M, TPA, and MHET concentrations; comparison of side chain interactions; DSC curves of PET fiber, PET/cotton, and PET/PU blended fibers; and summary of activity and productivity of PET hydrolases (PDF)

■ AUTHOR INFORMATION

Corresponding Author

Akihiko Nakamura − *Institute for Molecular Science, National Institutes of Natural Sciences, Okazaki 444-8787 Aichi, Japan; Department of Applied Life Sciences, Faculty of Agriculture and Research Institute of Green Science and Technology, Shizuoka University, Shizuoka 422-8529, Shizuoka, Japan;* orcid.org/0000-0003-0409-5759; Email: aki-naka@shizuoka.ac.jp

Authors

Takashi Matsuzaki − *Kirin Central Research Institute, Kirin Holdings Company, Limited, Fujisawa 251-8555 Kanagawa, Japan*

Toshiyuki Saeki − *Kirin Central Research Institute, Kirin Holdings Company, Limited, Fujisawa 251-8555 Kanagawa, Japan*

Fuhito Yamazaki − *Kirin Central Research Institute, Kirin Holdings Company, Limited, Fujisawa 251-8555 Kanagawa, Japan*

Natsuka Koyama − *Kirin Central Research Institute, Kirin Holdings Company, Limited, Fujisawa 251-8555 Kanagawa, Japan*

Tatsunori Okubo − *Institute for Packaging Innovation, Kirin Holdings Company, Limited, Yokohama 230-8628 Kanagawa, Japan*

Daiki Hombe − *Institute for Packaging Innovation, Kirin Holdings Company, Limited, Yokohama 230-8628 Kanagawa, Japan*

Yui Ogura − *Department of Agriculture, Graduate School of Integrated Science and Technology, Shizuoka University, Shizuoka 422-8529, Shizuoka, Japan*

Yoshihito Hashino − *Department of Agriculture, Graduate School of Integrated Science and Technology, Shizuoka University, Shizuoka 422-8529, Shizuoka, Japan*

Rie Tatsumi-Koga − *Advanced Data Science Center for Protein Research (ASPiRE), Institute for Protein Research (IPR), The University of Osaka, Osaka 565-0871, Japan;* orcid.org/0000-0002-5068-1049

Nobuyasu Koga − *Advanced Data Science Center for Protein Research (ASPiRE), Institute for Protein Research (IPR), The University of Osaka, Osaka 565-0871, Japan; Exploratory Research Center on Life and Living Systems (ExCELLS), National Institutes of Natural Sciences, Okazaki 444-8787 Aichi, Japan*

Ryota Iino − *Institute for Molecular Science, National Institutes of Natural Sciences, Okazaki 444-8787 Aichi, Japan; Graduate Institute for Advanced Studies, SOKENDAI, Hayama 240-0193 Kanagawa, Japan;* orcid.org/0000-0003-0110-5704

Complete contact information is available at: https://pubs.acs.org/10.1021/acssuschemeng.5c01602

Author Contributions

♦T.M. and T.S. contributed equally to this work. The manuscript was written through the contributions of all authors. All the authors approved the final version of the manuscript.

Notes

The authors declare no competing financial interest.

■ ACKNOWLEDGMENTS

This study was supported by the MEXT Leading Initiative for Excellent Young Researchers Grant Number 201990171, Grants-in-Aid for Scientific Research 24K01990 (to A.N.) from the Ministry of Education, Culture, Sports, Science, and Technology of Japan, and the JST FOREST Program (Grant Number JPMJFR210C, Japan).

■ ABBREVIATIONS

BHET, bis(2-hydroxyethyl) terephthalate; BMGY, buffered glycerol complex; BSM, basal salt medium; CD, circular dichroism; DO, dissolved oxygen; DSC, differential scanning calorimetry; EG, ethylene glycol; HSA, human serum albumin; IPTG, isopropyl *β*-*d*-1-thiogalactopyranoside; MES, 2-(N-morpholino) ethanesulfonic acid; MHET, mono-2-hydrox-

https://doi.org/10.1021/acssuschemeng.5c01602
ACS Sustainable Chem. Eng. 2025, 13, 10404−10417

yethyl terephthalate; MOPS, 3-(N-morpholino) propanesulfonic acid; PCR, polymerase chain reaction; PET, polyethylene terephthalate; pNO, 4-nitrophenyl octanoate; PU, polyurethane; qPCR, quantitative polymerase chain reaction; SOC, super optimal broth with catabolite repression; TPA, terephthalic acid; T_m, melting temperature; WT, wild-type; YPD, yeast extract, peptone, dextrose

REFERENCES

(1) Nisticò, R. Polyethylene terephthalate (PET) in the packaging industry. *Polym. Test.* **2020**, *90*, 106707.

(2) Geyer, R. Production, use, and fate of synthetic polymers; *Plastic Waste and Recycling*; Elsevier, 2020..

(3) Jaffe, M.; Easts, A. J.; Feng, X. Polyester fibers; *Thermal Analysis of Textiles and Fibers*; Elsevier, 2020..

(4) Morgan, L. R.; Birtwistle, G. An investigation of young fashion consumers' disposal habits. *Int. J. Consum. Stud* **2009**, *33* (2), 190−198.

(5) Šajn, N. Environmental impact of the textile and clothing industry What consumers need to know. European Parliamentary Research Service 2019. https://www.europarl.europa.eu/RegData/etudes/BRIE/2019/633143/EPRS_BRI(2019)633143_EN.pdf.

(6) Sahimaa, O.; Miller, E. M.; Halme, M.; Niinimäki, K.; Tanner, H.; Mäkelä, M.; Rissanen, M.; Härri, A.; Hummel, M. The only way to fix fast fashion is to end it. *Nat. Rev. Earth Environ* **2023**, *4* (3), 137−138.

(7) Palme, A.; Peterson, A.; de la Motte, H.; Theliander, H.; Brelid, H. Development of an efficient route for combined recycling of PET and cotton from mixed fabrics. *Textiles and Clothing Sustainability* **2017**, *3* (1), 4.

(8) Kaabel, S.; Arciszewski, J.; Borchers, T. H.; Therien, J. P. D.; Friščić, T.; Auclair, K. Solid-State Enzymatic Hydrolysis of Mixed PET/Cotton Textiles. *ChemSusChem* **2023**, *16* (1), No. e202201613.

(9) Morley, N.; Slater, S.; Russell, S.; Tipper, M.; Ward, G. D. *Recycling of Low Grade Clothing Waste*. Oakdene Hollins Ltd, Salvation Army Trading Company Ltd Nonwovens Innovation & Research Institute Ltd, 2006. http://www.inno-therm.com/wp-content/uploads/2013/10/Recycle-Low-Grade-Clothing.pdf (accessed 2024 31 October 2024).

(10) Ragaert, K.; Delva, L.; Van Geem, K. Mechanical and chemical recycling of solid plastic waste. *Waste Manag* **2017**, *69*, 24−58.

(11) Muringayil Joseph, T.; Azat, S.; Ahmadi, Z.; Moini Jazani, O.; Esmaeili, A.; Kianfar, E.; Haponiuk, J.; Thomas, S. Polyethylene terephthalate (PET) recycling: A review. *Case Stud Chem Environ Eng* **2024**, *9*, 100673.

(12) Cao, F.; Wang, L.; Zheng, R.; Guo, L.; Chen, Y.; Qian, X. Research and progress of chemical depolymerization of waste PET and high-value application of its depolymerization products. *RSC Adv.* **2022**, *12* (49), 31564−31576.

(13) Bohre, A.; Jadhao, P. R.; Tripathi, K.; Pant, K. K.; Likozar, B.; Saha, B. Chemical Recycling Processes of Waste Polyethylene Terephthalate Using Solid Catalysts. *ChemSusChem* **2023**, *16* (14), No. e202300142.

(14) Pham, D. D.; Cho, J. Low-energy catalytic methanolysis of poly(ethyleneterephthalate). *Green Chem.* **2021**, *23* (1), 511−525.

(15) Tollini, F.; Brivio, L.; Innocenti, P.; Sponchioni, M.; Moscatelli, D. Influence of the catalytic system on the methanolysis of polyethylene terephthalate at mild conditions: A systematic investigation. *Chem. Eng. Sci.* **2022**, *260*, 117875.

(16) Tanaka, S.; Sato, J.; Nakajima, Y. Capturing ethylene glycol with dimethyl carbonate towards depolymerisation of polyethylene terephthalate at ambient temperature. *Green Chem.* **2021**, *23* (23), 9412−9416.

(17) Zhang, S.; Xu, W.; Du, R.; Zhou, X.; Liu, X.; Xu, S.; Wang, Y.-Z. Cosolvent-promoted selective non-aqueous hydrolysis of PET wastes and facile product separation. *Green Chem.* **2022**, *24* (8), 3284−3292.

(18) Uekert, T.; Singh, A.; DesVeaux, J. S.; Ghosh, T.; Bhatt, A.; Yadav, G.; Afzal, S.; Walzberg, J.; Knauer, K. M.; Nicholson, S. R.; et al. Technical, Economic, and Environmental Comparison of Closed-Loop Recycling Technologies for Common Plastics. *ACS Sustainable Chem. Eng.* **2023**, *11* (3), 965−978.

(19) Kawai, F.; Iizuka, R.; Kawabata, T. Engineered polyethylene terephthalate hydrolases: perspectives and limits. *Appl. Microbiol. Biotechnol.* **2024**, *108* (1), 404.

(20) Martínez, A.; Maicas, S. Cutinases: Characteristics and Insights in Industrial Production. *Catalysts* **2021**, *11* (10), 1194.

(21) Müller, R. J.; Schrader, H.; Profe, J.; Dresler, K.; Deckwer, W. D. Enzymatic Degradation of Poly(ethylene terephthalate): Rapid Hydrolyse using a Hydrolase from T. fusca. *Macromol. Rapid Commun.* **2005**, *26* (17), 1400−1405.

(22) Tournier, V.; Topham, C. M.; Gilles, A.; David, B.; Folgoas, C.; Moya-Leclair, E.; Kamionka, E.; Desrousseaux, M. L.; Texier, H.; Gavalda, S.; et al. An engineered PET depolymerase to break down and recycle plastic bottles. *Nature* **2020**, *580* (7802), 216−219.

(23) Zheng, Y.; Li, Q.; Liu, P.; Yuan, Y.; Dian, L.; Wang, Q.; Liang, Q.; Su, T.; Qi, Q. Dynamic Docking-Assisted Engineering of Hydrolases for Efficient PET Depolymerization. *ACS Catal.* **2024**, *14* (5), 3627−3639.

(24) Son, H. F.; Cho, I. J.; Joo, S.; Seo, H.; Sagong, H.-Y.; Choi, S. Y.; Lee, S. Y.; Kim, K.-J. Rational Protein Engineering of Thermo-Stable PETase from Ideonella sakaiensis for Highly Efficient PET Degradation. *ACS Catal.* **2019**, *9* (4), 3519−3526.

(25) Cui, Y.; Chen, Y.; Liu, X.; Dong, S.; Tian, Y. e.; Qiao, Y.; Mitra, R.; Han, J.; Li, C.; Han, X.; et al. Computational Redesign of a PETase for Plastic Biodegradation under Ambient Condition by the GRAPE Strategy. *ACS Catal.* **2021**, *11* (3), 1340−1350.

(26) Lu, H.; Diaz, D. J.; Czarnecki, N. J.; Zhu, C.; Kim, W.; Shroff, R.; Acosta, D. J.; Alexander, B. R.; Cole, H. O.; Zhang, Y.; et al. Machine learning-aided engineering of hydrolases for PET depolymerization. *Nature* **2022**, *604* (7907), 662−667.

(27) Bell, E. L.; Smithson, R.; Kilbride, S.; Foster, J.; Hardy, F. J.; Ramachandran, S.; Tedstone, A. A.; Haigh, S. J.; Garforth, A. A.; Day, P. J. R.; et al. Directed evolution of an efficient and thermostable PET depolymerase. *Nat. Catal* **2022**, *5* (8), 673−681.

(28) Cui, Y.; Chen, Y.; Sun, J.; Zhu, T.; Pang, H.; Li, C.; Geng, W. C.; Wu, B. Computational redesign of a hydrolase for nearly complete PET depolymerization at industrially relevant high-solids loading. *Nat. Commun.* **2024**, *15* (1), 1417.

(29) Arnal, G.; Anglade, J.; Gavalda, S.; Tournier, V.; Chabot, N.; Bornscheuer, U. T.; Weber, G.; Marty, A. Assessment of Four Engineered PET Degrading Enzymes Considering Large-Scale Industrial Applications. *ACS Catal.* **2023**, *13* (20), 13156−13166.

(30) Meilleur, C.; Hupe, J. F.; Juteau, P.; Shareck, F. Isolation and characterization of a new alkali-thermostable lipase cloned from a metagenomic library. *J. Ind. Microbiol. Biotechnol.* **2009**, *36* (6), 853−861.

(31) Secundo, F.; Carrea, G.; Tarabiono, C.; Gatti-Lafranconi, P.; Brocca, S.; Lotti, M.; Jaeger, K.-E.; Puls, M.; Eggert, T. The lid is a structural and functional determinant of lipase activity and selectivity. *J. Mol. Catal. B: Enzym.* **2006**, *39* (1−4), 166−170.

(32) Danso, D.; Schmeisser, C.; Chow, J.; Zimmermann, W.; Wei, R.; Leggewie, C.; Li, X.; Hazen, T.; Streit, W. R. New Insights into the Function and Global Distribution of Polyethylene Terephthalate (PET)-Degrading Bacteria and Enzymes in Marine and Terrestrial Metagenomes. *Appl. Environ. Microbiol.* **2018**, *84* (8), No. e02773.

(33) Nakamura, A.; Kobayashi, N.; Koga, N.; Iino, R. Positive Charge Introduction on the Surface of Thermostabilized PET Hydrolase Facilitates PET Binding and Degradation. *ACS Catal.* **2021**, *11* (14), 8550−8564.

(34) Nakamura, A.; Tasaki, T.; Okuni, Y.; Song, C.; Murata, K.; Kozai, T.; Hara, M.; Sugimoto, H.; Suzuki, K.; Watanabe, T.; et al. Rate constants, processivity, and productive binding ratio of Chitinase A revealed by single-molecule analysis. *Phys. Chem. Chem. Phys.* **2018**, *20* (5), 3010−3018.

(35) Molitor, R.; Bollinger, A.; Kubicki, S.; Loeschcke, A.; Jaeger, K. E.; Thies, S. Agar plate-based screening methods for the identification

https://doi.org/10.1021/acssuschemeng.5c01602
ACS Sustainable Chem. Eng. 2025, 13, 10404−10417

of polyester hydrolysis by Pseudomonas species. *Microb Biotechnol* **2020**, *13* (1), 274−284.
(36) Abramson, J.; Adler, J.; Dunger, J.; Evans, R.; Green, T.; Pritzel, A.; Ronneberger, O.; Willmore, L.; Ballard, A. J.; Bambrick, J.; et al. Accurate structure prediction of biomolecular interactions with AlphaFold 3. *Nature* **2024**, *630* (8016), 493−500.
(37) Jurrus, E.; Engel, D.; Star, K.; Monson, K.; Brandi, J.; Felberg, L. E.; Brookes, D. H.; Wilson, L.; Chen, J.; Liles, K.; et al. Improvements to the APBS biomolecular solvation software suite. *Protein Sci.* **2018**, *27* (1), 112−128.
(38) Kasturi, L.; Eshleman, J. R.; Wunner, W. H.; Shakin-Eshleman, S. H. The hydroxy amino acid in an Asn-X-Ser/Thr sequon can influence N-linked core glycosylation efficiency and the level of expression of a cell surface glycoprotein. *J. Biol. Chem.* **1995**, *270* (24), 14756−14761.
(39) Shirke, A. N.; White, C.; Englaender, J. A.; Zwarycz, A.; Butterfoss, G. L.; Linhardt, R. J.; Gross, R. A. Stabilizing Leaf and Branch Compost Cutinase (LCC) with Glycosylation: Mechanism and Effect on PET Hydrolysis. *Biochemistry* **2018**, *57* (7), 1190−1200.
(40) Austin, H. P.; Allen, M. D.; Donohoe, B. S.; Rorrer, N. A.; Kearns, F. L.; Silveira, R. L.; Pollard, B. C.; Dominick, G.; Duman, R.; El Omari, K.; et al. Characterization and engineering of a plastic-degrading aromatic polyesterase. *Proc. Natl. Acad. Sci. U.S.A.* **2018**, *115* (19), E4350−E4357.
(41) Chen, C.-C.; Han, X.; Li, X.; Jiang, P.; Niu, D.; Ma, L.; Liu, W.; Li, S.; Qu, Y.; Hu, H.; et al. General features to enhance enzymatic activity of poly(ethylene terephthalate) hydrolysis. *Nat. Catal* **2021**, *4* (5), 425−430.
(42) Chen, C. C.; Han, X.; Ko, T. P.; Liu, W.; Guo, R. T. Structural studies reveal the molecular mechanism of PETase. *FEBS J.* **2018**, *285* (20), 3717−3723.
(43) Han, X.; Liu, W.; Huang, J. W.; Ma, J.; Zheng, Y.; Ko, T. P.; Xu, L.; Cheng, Y. S.; Chen, C. C.; Guo, R. T. Structural insight into catalytic mechanism of PET hydrolase. *Nat. Commun.* **2017**, *8* (1), 2106.
(44) Burgin, T.; Pollard, B. C.; Knott, B. C.; Mayes, H. B.; Crowley, M. F.; McGeehan, J. E.; Beckham, G. T.; Woodcock, H. L. The reaction mechanism of the Ideonella sakaiensis PETase enzyme. *Commun. Chem.* **2024**, *7* (1), 65.
(45) Ogura, Y.; Hashino, Y.; Nakamura, A. Direct Screening of PET Hydrolase Activity in Culture Medium Based on Turbidity Reduction. *ACS Omega* **2024**, *9* (31), 34151−34160.
(46) Deng, B.; Yue, Y.; Yang, J.; Yang, M.; Xing, Q.; Peng, H.; Wang, F.; Li, M.; Ma, L.; Zhai, C. Improving the activity and thermostability of PETase from Ideonella sakaiensis through modulating its post-translational glycan modification. *Commun. Biol.* **2023**, *6* (1), 39.
(47) Li, X.; Shi, B.; Huang, J. W.; Zeng, Z.; Yang, Y.; Zhang, L.; Min, J.; Chen, C. C.; Guo, R. T. Functional tailoring of a PET hydrolytic enzyme expressed in Pichia pastoris. *Bioresour Bioprocess* **2023**, *10* (1), 26.
(48) Chen, C.-C.; Li, X.; Min, J.; Zeng, Z.; Ning, Z.; He, H.; Long, X.; Niu, D.; Peng, R.; Liu, X.; et al. Complete decomposition of poly(ethylene terephthalate) by crude PET hydrolytic enzyme produced in Pichia pastoris. *Chem. Eng. J.* **2024**, *481*, 148418.
(49) Shu, M.; Shen, W.; Yang, S.; Wang, X.; Wang, F.; Wang, Y.; Ma, L. High-level expression and characterization of a novel serine protease in Pichia pastoris by multi-copy integration. *Enzyme Microb. Technol.* **2016**, *92*, 56−66.
(50) Xi, X.; Ni, K.; Hao, H.; Shang, Y.; Zhao, B.; Qian, Z. Secretory expression in Bacillus subtilis and biochemical characterization of a highly thermostable polyethylene terephthalate hydrolase from bacterium HR29. *Enzyme Microb. Technol.* **2021**, *143*, 109715.
(51) Chen, X. Q.; Rao, D. M.; Zhou, X. Y.; Li, Y.; Zhao, X. M.; Kong, D. M.; Xu, H.; Feng, C. Q.; Wang, L.; Su, L. Q.; et al. Enhancement of the yield of poly (ethylene terephthalate) hydrolase production using cell membrane protection strategy. *Bioresour. Technol.* **2025**, *418*, 131903.
(52) Wu, T.; Sun, H.; Wang, W.; Xie, B.; Wang, Z.; Lu, J.; Xu, A.; Dong, W.; Zhou, J.; Jiang, M. Boosting extracellular FastPETase production in E. coli: A combined approach of cognate chaperones co-expression and vesicle nucleating peptide tag fusion. *Int. J. Biol. Macromol.* **2024**, *283* (Pt 3), 137857.
(53) Barth, M.; Oeser, T.; Wei, R.; Then, J.; Schmidt, J.; Zimmermann, W. Effect of hydrolysis products on the enzymatic degradation of polyethylene terephthalate nanoparticles by a polyester hydrolase from Thermobifida fusca. *Biochem. Eng. J.* **2015**, *93*, 222−228.
(54) Pfaff, L.; Gao, J.; Li, Z.; Jackering, A.; Weber, G.; Mican, J.; Chen, Y.; Dong, W.; Han, X.; Feiler, C. G.; et al. Multiple Substrate Binding Mode-Guided Engineering of a Thermophilic PET Hydrolase. *ACS Catal.* **2022**, *12* (15), 9790−9800.
(55) Farah, S.; Tsach, T.; Bentolila, A.; Domb, A. J. Morphological, spectral and chromatography analysis and forensic comparison of PET fibers. *Talanta* **2014**, *123*, 54−62.
(56) Yang, B.; Min Huang, W.; Li, C.; Hoe Chor, J. Effects of moisture on the glass transition temperature of polyurethane shape memory polymer filled with nano-carbon powder. *Eur. Polym. J.* **2005**, *41* (5), 1123−1128.

https://doi.org/10.1021/acssuschemeng.5c01602
ACS Sustainable Chem. Eng. 2025, 13, 10404−10417